RESEARCH ARTICLE

THEORETICAL STUDY OF STRUCTURE AND PROPERTIES OF Ni$_2$MnGa HEUSLER ALLOY

[1]ShanmugaSundari, R. and [2]Manickam Mahendran[2]

[1] Department of Physics, Stella Maris College, Chennai- 600 086, India.
[2]Smart Materials Laboratory, Department of Physics, Thiagarajar College of Engineering,
Madurai – 625 015, India

ARTICLE INFO

ABSTRACT

The structure determination of Ferromagnetic Shape Memory Alloy Ni$_2$MnGa is a major challenge. This paper reports the investigation of the structure and properties of Ni$_2$MnGa Heusler alloy from the theoretical point of view using ab-initio and density-functional calculations through Gaussian.

INTRODUCTION

Actuator materials can be used to control aerodynamic devices, valves in automotive systems and sensors. These materials can ultimately facilitate the replacement of complex mechanical systems. Actuators respond to a controlled external influence, generating large amounts of strain. Light actuators that have extended lifetimes, and have high response frequencies under accurate control are favourable. Among currently available actuator materials, Ni$_2$MnGa Ferromagnetic shape memory alloy (FSMA) show considerable potential to meet the required demands. Its unique character is the greater strain it shows as compared to other magnetostrictive materials. Ni$_2$MnGa therefore is a material on which extensive research can be done. Summary of the study of Ni$_2$MnGa by various researchers is outlined. Ni–Mn–Ga was first shown to produce significant strains (Ullakko *et al.,* 1996) and the alloy was found to have low hysteresis, large strains ~up to 10%, and a transition temperature that is adjustable with composition (Sozinov *et al.,* 2002). The equilibrium lattice constants and calculated magnetic moments by means of the FLAPW method were found to be in good agreement with experimental data (Ayuela *et al.,* 1999). The possibility of martensitic transformations was studied by making tetragonal and orthorhombic distortions to the cubic structure with the volume fixed to the equilibrium value. Electronic aspects of the distortion were explained and the

---

*Corresponding author: shsundari@gmail.com

DOS splitting calculations around the Fermi level were studied with the density-functional theory using FLAPW method via WIEN code (Ayuela *et al.,* 2002). The effective value of the splitting was found to be proportional to the deformation in ab-initio study of tetragonal variants in Ni$_2$MnGa alloy. A simple statistical model was proposed for the effective computer simulation of the main features of stress–strain–temperature super elastic behaviour observed in Ni–Mn–Ga alloys (Chernenko *et al.,* 2004). Another model for temperature dependence of field-induced strain in ferromagnetic shape memory alloys was devised (Robert Handley *et al.,* 2006). The magnetic torque on the crystal was suggested to be the driving force for twin-boundary motion. Ginzburg–Landau description was made for phase transitions in Ni–Mn–Ga system using first-principles calculations using VASP and KKR CPA (Entel *et al.,* 2006). They analysed magnetic, phonon and electronic properties of a series of Heusler compounds and explained the reason for the martensitic instabilities of Ni-based alloys. The compositional dependence of the martensitic transition temperature was correlated to the valence electron concentration *e/a*.

The equilibrium structure and electronic properties of Ni$_2$MnGa for both the martensitic and austenitic phases were studied by full potential linearized augmented plane wave method (Barman *et al.,* 2005). The *ab initio*, relativistic, and spin-polarized FPLAPW calculations were performed with generalized gradient approximation for the exchange correlation using the WIEN97 code.

Extensive studies using experimental methods were carried out by many researchers for structure determination and performance of these alloys. The martensitic transformation and the magnetic properties of the alloys were found to depend strongly on Mn/Ga ratio and on the annealing temperature (Singh *et al.,* 2008). With increase in Mn substitution for Ga, martensite transformation temperature increased, while the Curie temperature and magnetization values decreased. This was attributed to the e/a ratio of the alloys. A thermodynamic model for the sensing effect was formulated that quantified the stress and dependence of magnetization on strain of Ni–Mn–Ga (Sarawate, 2007). Another such model was presented in which the microstructure of single-crystal Ni–Mn–Ga was represented by internal state variables, and evolution of these variables was used to quantify the strain and magnetization response to applied magnetic fields (Hirsinger and Lexcellent., 2004).

The mechanisms of the magnetic microstructure, which cause the martensite band domains to run diagonally in a micrograph from left to right was observed (Manickam Mahendran., 2005). Martensitic transformation of Ni–24.7Mn–24.8 Ga (at.%) alloy not only depend on the structural rearrangement but was also found to respond to magnetic field. Effects of first neighbour ordering and second neighbour ordering on the martensitic transformation and the Curie temperatures of Ni_2MnGa alloys were studied (Hideki Hosoda et al ., 2000). It was found that the degree of second neighbour ordering lowered with increase in heat treatment temperature. Density Functional Theory code CASTEP was used to analyse optical properties of Ni–Mn–Ga and it confirmed the structural dependence of these properties (Wan *et al.,* 2005). Experiments were carried out in a wide temperature range using high magnetic field and reported martensitic transition temperature increase and pre-martensitic transition temperature decrease with application of magnetic fields up to 2 T. The transition temperatures do not change in fields up to 5 T (Awaji *et al.,* 2000). In spite of widespread experimental and theoretical research on FSMA, the structural search of Ni-Mn-Ga for their variants is a major challenge. The present study aims at using robust computing techniques of Gaussian for structure determination and prediction of properties (Frisch *et al.,* 2004).

Computational method

Gaussian 03 is an electronic structure program used by chemists, biochemists, physicists and others for research in emerging areas of chemical interest. Starting from the basic laws of quantum mechanics, *Gaussian* predicts the energies and molecular structures along with numerous molecular properties derived from the basic computation types. It can be used to study molecules and reactions under a wide range of conditions, including both stable species and compounds which are difficult or impossible to observe experimentally. Short-lived intermediates and transition structures can be studied by Gaussian. In our study both Hartree-Fock (HF) and DFT (B3LYP) theories are used. Powder Cell for Windows is an excellent Graphical user interface based program for the investigation and display of crystal structures. By the use of crystallographic and crystal chemical knowledge, Powder Cell helps to create a new

crystal structure in a relatively short time. The generated structure for the material under study is shown in Figure 1.The molecular specification of Ni_2MnGa FSMA that is to be fed to Gaussian, is arrived at using Powder Cell**.**
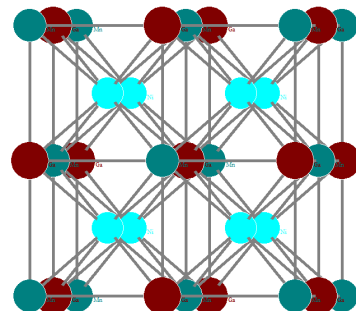

Fig.1: Structure of Ni_2MnGa as generated by Powder Cell

The magnetic properties and structures of Ni_2MnGa have been studied by means of X-ray and neutron diffraction measurements (Webster *et al.,* 1972 and 1973). The alloy shows ordered face centred cubic Heusler structure shown in Figure1, with ferromagnetic ordering. In this paper, the simulations deal with the simplest structure unit of the material, the unit cell containing nine atoms is presented in Figure 2. Space group number used is 225.
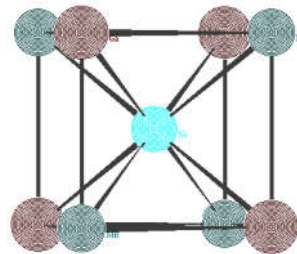

Fig. 2: Unit cell of $L2_1$ cubic Ni_2MnGa

It is desirable to optimize the molecular geometry before calculating molecular properties, however ab initio geometry optimization is impractical for large molecules. It is normal to be content with Single point calculations done with geometry arrived at experimentally or theoretically. In the present study, we have calculated E_{tot} by varying the *lattice constant, for* the cubic austenitic phase. The Cartesian coordinates generated through Powder Cell were used in Gaussian and the results of Gaussian output are shown in Table 1 for various 'a'. Every *Gaussian* job must specify both a method and a basis set. Two different methods used in the study are HF and DFT and basis sets are 3-21G, 6-31G* and 6-31G**. The simplest basis set 3-21G gives reasonable results. 6-31G* adds polarization to all atoms, and improves the modelling of core electrons. It is often considered the best compromise of speed and accuracy. The most commonly used basis set 6-31G** can improve the total energy of the system. Very large basis sets have a difficulty in converging and thus require tighter tolerances.
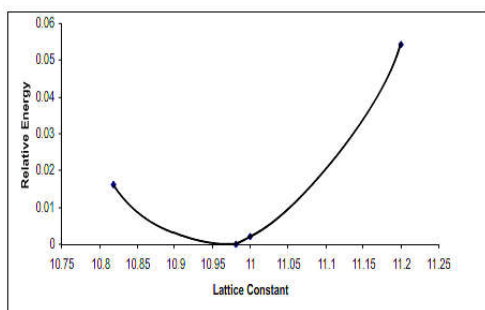
RESULTS AND DISCUSSION

Gaussian outputs for various lattice constants of the cubic austenitic phase of Ni_2MnGa are listed in the Table 1.

Table 1. Theoretical Energy. (in hartrees).

For a=5.823 A°

BASIS SET	SCF ENERGY (#HF)	DFT ENERGY (#B3LYP)
3-21G	-13730.7420892	-13744.21344
6-31G	-13788.9047466	-13802.67749
6-31+G*	-13789.41526	-13803.2952809

For a=5.811 A°

6-31G	-13788.904702	-13802.6800754
6-31G*	--	-13803.069168
6-31G**	-13789.2192526 †	-13803.0691683 ††

For a=5.725 A°

6-31G*	-13789.2290700	-13803.0529612
6-31G**	-13789.2290700	-13803.0529612

For a=6.08557A°

JOB TYPE	ENERGY	
#HF/6-31G**	-13789.2124803	
#B3LYP6-31G**	-13803.0089828	

† Value of SCF Energy obtained by Breczko et al for the same system was -13797.099 hartrees. †† DFT Energy obtained was -13774.816 hatrees using computational package NWChem.

The total DFT energy is calculated as a function of the lattice parameter, and plotted in Figure 3 to optimize the $L2_1$ structure of ferromagnetic Ni_2MnGa Heusler alloy.

Fig.3. Relative energy of Ni_2MnGa Heusler alloy as a function of lattice constant

The present study shows the equilibrium lattice constant to be 5.811 A° (10.981 a.u.). This is in good agreement with results of neutron and x-ray diffraction measurements and previous theoretical studies (Wedel *et al.,* 1999 and Biswas *et al.,* 2002). Ayuela et al has found the theoretical lattice constant using FLAPW method to be 5.811 A° (10.981 a.u.) which is perfectly identical to the current finding. The experimental value arrived by them was 11.01a.u. Ozdemir et al carried out spin-polarized total energy calculations by using the Vienna ab initio simulation package (VASP) and the implemented projector augmented wave pseudopotential formalism (PAW) and reported a=5.812 A°. For the cubic austenitic phase, Barman et al calculated the equilibrium lattice constant to be 10.998 a.u. (5.820 A°) and they have reported 11.004 a.u. from their x-ray diffraction measurements.

Vibrational analysis

IR study for organic molecules are reported extensively in literature. Inorganic analysis is less researched since their vibrational spectra are too weak, more difficult to obtain and do not appear in common middle infrared egion (4000 - 400 cm^{-1}) but emerge in far infrared region (under 400 cm^{-1}). The vibrational frequency calculations for Ni_2MnGa at B3LYP and HF levels using the 6-31G(d,p) basis set have been summarized in Tables 2 and 3 and the corresponding IR spectra are shown in Figures 4 and 5 respectively. The vibrations of atoms responsible for the peaks in the spectrum are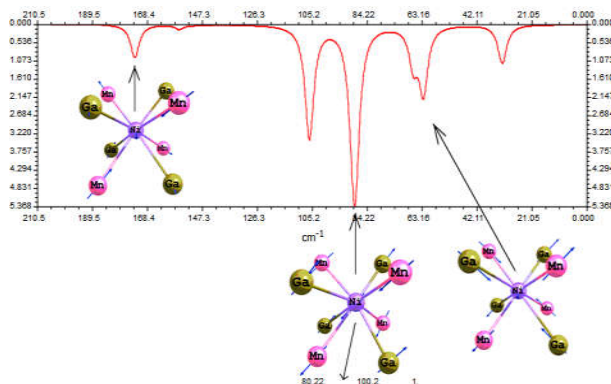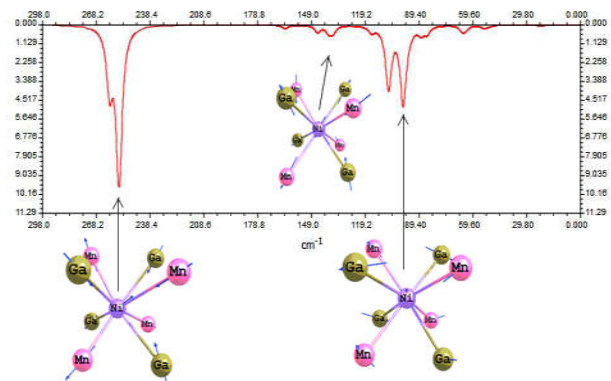 shown. The displacement vectors indicate bending vibrations in lower frequencies and stretching vibrations in higher range. GaussView program was used in visualising the output.

Table 2. Vibrational study of Ni_2MnGa using B3LYP /6-31G [frequency (cm^{-1}) IR intensities(km mol^{-1}), reduced mass amu) and force constants (m dyn $°A^{-1}$)]**

Sl. No	Frequency	IR intensity	Reduced Mass	Force const.
1	16.0481	0.0031	60.3744	0.0092
2	32.8679	0.5378	57.7714	0.0368
3	62.7671	0.9955	65.1909	0.1513
4	66.6875	1.0891	67.4739	0.1768
5	88.8383	2.9126	60.7840	0.2826
6	89.6750	2.6201	60.6477	0.2873
7	97.8416	0.0043	63.2436	0.3567
8	106.5275	3.3323	59.0248	0.3946
9	126.7584	0.0002	55.6199	0.5265
10	156.4372	0.1335	56.4097	0.8134
11	173.4384	0.9752	57.5697	1.0203

Table 3. Vibrational study of Ni_2MnGa using HF /6-31G [frequency (cm^{-1}) IR intensities(km mol^{-1}), Raman scattering activities ($°A$ amu^{-1}), reduced mass (amu) and force constants (m dyn $°A^{-1}$)]**

Sl. No	Frequency	IR intensity	Raman Activ	Reduced Mass	Force const.
1	22.0544	0.0868	6.6465	57.5612	0.0165
2	43.0559	0.0058	2.1092	58.5269	0.0639
3	50.5693	0.0817	1.4595	59.4540	0.0896
4	53.6333	0.1984	1.5161	56.9925	0.0966
5	63.7581	0.2405	9.2775	60.6026	0.1451
6	85.1729	0.4346	6.4246	63.5375	0.2716
7	95.2742	0.2587	45.6307	65.0635	0.3480
8	98.4186	4.6357	6.4299	64.4114	0.3676
9	106.5082	3.7125	2.2322	63.1382	0.4220
10	137.1834	0.3809	0.1215	62.0912	0.6885
11	145.8015	0.4235	6.2353	60.8687	0.7624
12	256.0920	5.2919	22.9255	57.4859	2.2213
13	261.0767	3.6228	10.9584	57.5590	2.3115

Fig. 4. Infrared spectra of Ni_2MnGa using B3LYP/6–31G method**

Fig. 5. Infrared spectra of Ni_2MnGa using HF/6–31G method**

Intrinsic Reaction Coordinate study for Ni₂MnGa

The path of a chemical reaction can be traced from the Transition State to the products and/or to the reactants, using the Intrinsic Reaction Coordinate method (IRC). The IRC path is defined as the steepest-descent path from the Transition State down to the local energy minimum. The energy profile is obtained as well as the length and curvature properties of the path, providing the basic quantities for an analysis of reaction path.   Energies are reported relative to the Transition State energy of -13803.059442 hatrees in Table 4 and traced in Figure 6.

Table 4. Summary of reaction path for Ni₂MnGa

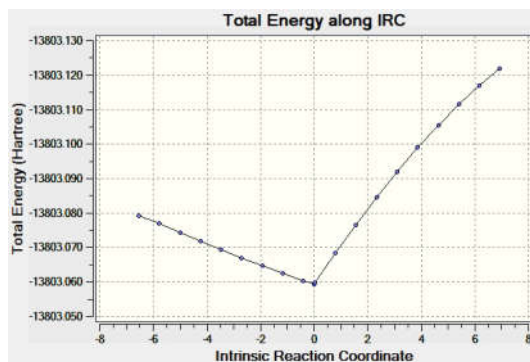|	Energy	Rx Coord
1	-0.01976	-6.54173
2	-0.01742	-5.77627
3	-0.01498	-5.00904
4	-0.01248	-4.24140
5	-0.01000	-3.47366
6	-0.00760	-2.70635
7	-0.00529	-1.93911
8	-0.00309	-1.17190
9	-0.00099	-0.40582
10	-0.00001	-0.00146
11	0.00000	0.00000
12	-0.00026	0.02976
13	-0.00886	0.79715
14	-0.01713	1.56456
15	-0.02502	2.33195
16	-0.03249	3.09933
17	-0.03953	3.86669
18	-0.04607	4.63402
19	-0.05210	5.40130
20	-0.05758	6.16852
21	-0.06249	6.93562

Fig. 6. Intrinsic Reaction Coordinate path of Ni₂MnGa

Other molecular properties

On the basis of vibrational analysis using B3LYP/6-31G** and HF/6-31G** methods, several thermodynamic parameters are calculated and are presented in Table 5. The zero point vibration energies (ZPVE) and the entropy, S are calculated to the extent of accuracy and the variations seem to be insignificant. The total energies and the change in the total entropy of Ni₂MnGa at different methods are only marginal. As can be seen from the data, the thermal energy arises mainly from vibrational modes.

Thermo chemistry

In this section the results of thermo chemical calculations are reported. All computed results are at 298.15K and at 1 atm. pressure. The values of specific heat at constant volume (C_v) and entropy (S) found using B3LYP/6-31G**

job types are listed in Table 6. For the case of entropy translational, vibrational and rotational modes all have significant contributions.

Table 5. Theoretically computed energies (a.u.), zero-point vibrational energies (kcal mol⁻¹), rotational constants (GHz), Thermal Energies (Kcal Mol⁻¹), dipole moment (Debye) on the basis of vibrational analysis.

Parameters	HF/ 6-31G**	B3LYP/ 6-31G**
Total energy	-13789.2192526	-13803.0309545
Zero point energy	3.21300	4.84531
Rotational constants	0.24166	0.24166
	0.24166	0.24166
	0.24166	0.24166
Total	13.442	14.721
Translational	0.889	0.889
Rotational	0.889	0.889
Vibrational	11.665	12.944
Dipole moment	0.4114	0.0001

Table 6. Computed Specific heat at constant volume (C_v) and entropy (S) using B3LYP/6-31G method**

	Cv (cal/mol-K)	S (cal/mol-K)
Total	39.124	147.213
Electronic	0.000	0.000
Translational	2.981	44.818
Rotational	2.981	34.387
Vibrational	33.163	68.008

Visualization of Molecular Orbitals

Using MO Editor of GaussView, molecular Energies and Molecular Orbitals of Ni₂MnGa are calculated using DFT study and shown in Figure 7. The mesh view of Highest Occupied Molecular Orbital (HOMO) and Lowest Unoccupied Molecular Orbital (LUMO) are shown for the isovalue of 0.02. HOMO and LUMO output of HF calculations are shown in Fig 8.LUMO outputs of both methods are identical while HOMO varies. Isosurfaces of Ga atoms are found to be symmetric in both outputs and contribution of Mn atoms varies very much.
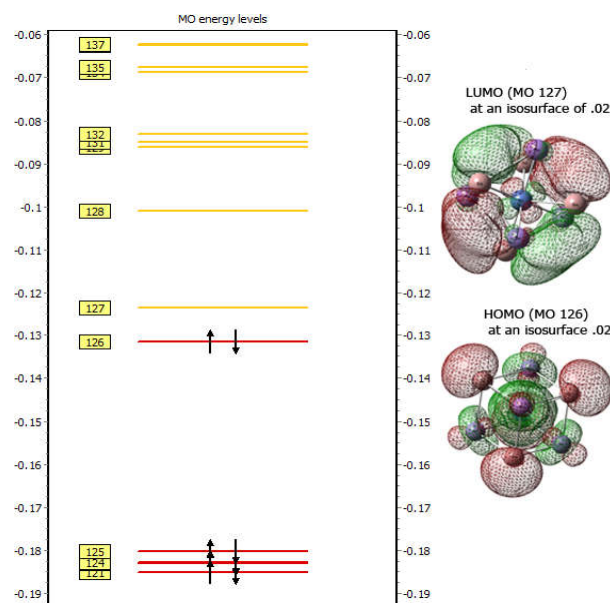

Fig. 7. Molecular Orbital Energy diagram of Ni₂MnGa with HOMO and LUMO view -DFT output

The charge distribution of the unit cell with display of Mulliken charges and Electrostatic Surface Potential (ESP) give better visualization and understanding. These graphics are shown in Figure 9 (a-d) where fig 9(b) is drawn with density=0.004, fig 9(c) with density=0.04 and fig 9(d) has mesh view. ESP pictures are meant to be qualitative in nature to highlight the locations of positive and negative charge. (Maximum negative charge is shown in Red and maximum positive in Blue and the intermediate charges in gradient colors).
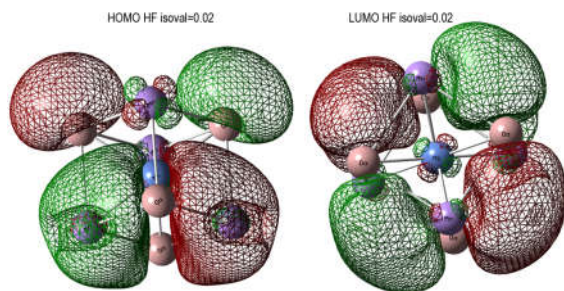

Fig. 8. MO diagram of Ni₂MnGa with HOMO and LUMO view –HF output

Similar isosurface study of electron density of the unit cell was reported by T. Breczko et al.. The results are associated with the 'd' electrons of Mn atoms of the unit cell, and their highest spin results in a 'cubic' form of density near Mn atoms. It is interesting to note the form of isosurface depends on the spin state of the unit cell. Electrostatic potential calculation made for isoval of 0.04, is displayed in Figure 10.
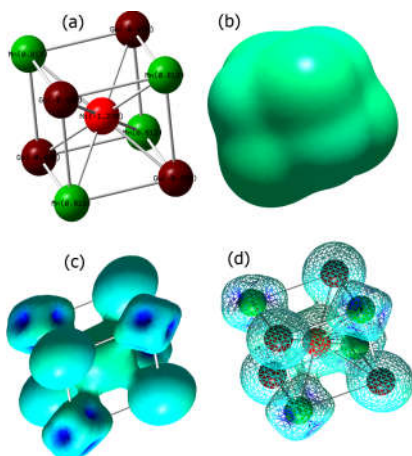

Fig. 9. Gauss View outputs (a) Ni₂MnGa unit cell showing Mulliken charges (b) Charge Density for isoval=0.004(c) for isoval=0.04 and (d)Mesh view
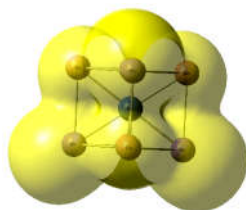

Fig. 10. Gaussview Electrostatic potential from Total SCF Density(isoval = 0.04)

Conclusions

Structure determination was done by ab initio and DFT simulation in Gaussian and the results were found to be in agreement with results in literature. Though Gaussian is used extensively by researchers, study of Ni₂MnGa FSMA using Gaussian was the first of its nature and it poses challenges like the need of high-speed processor. This study demonstrates that HF/DFT calculations using Gaussian offer a powerful approach in analysing the alloy Ni₂MnGa.Further analysis is in progress for the same system. Since Ni–Mn–Ga is one of the most promising candidates for producing field-driven actuators, we attempted the computational studies of Ni-Mn-Ga alloys. Theoretical studies help clarify the fundamental interactions that are responsible for their magnetic behaviour.

REFERENCES

Ayuela, A., Enkovaara, J. and Nieminen, RM. 2002. Ab initio study of tetragonal variants in Ni 2 MnGa alloy, *Journal of Physics: Condensed Matter,* 14: 5325–5336.

Ayuela, A., Enkovaara., J., Ullakko, K. and Nieminen, RM. 1999. Structural properties of magnetic Heusler alloys, *Journal of Physics: Condensed Matter*, 11:2017–2026.

Barman, S.R., Banik, S. and Aparna Chakrabarti, 2005. Structural and electronic properties of Ni₂MnGa. *Physical Review* B, 72, pp 184410-7.

Biswas, C., Okram, G.S., Awasthi, A. M., Lalla, N. P. and Barman, S. R. 2002. Transport and structural study of ferromagnetic shape memory alloy: $Ni_{2+x}Mn_{1-x}Ga$, Proceedings of DAE Solid State Physics Symposium, 45, pp 439.

Breczko, T., Barkaline, V.V., Grechishkin, R.M. and Nelayev, V.V. 2010. Magnetic properties of Ni₂MnGa alloy. *Materials Physics and Mechanics*, 9, pp 53-67.

Chernenko, V.A., L'vov, V.A., Cesari, E., Pons, J., Rudenko, A.A.,Date H.,Matsumoto, M. and Kanomata, T. 2004. Stress–strain behaviour of Ni–Mn–Ga alloys: experiment and modeling**,** Materials Science and Engineering A, 378 , pp 349–352.

Entel, P., Buchelnikov, V.D., Khovailo, V.V., Zayak, A. T., Adeagbo, W.A., Gruner, M.E., Herper, H.C. and Wassermann, E.F. 2006. Ab initio modeling of martensitic transformations (MT) in magnetic shape memory alloys. *Journal of Physics D: Applied Physics,* 39, pp 865–889.

Frisch, A., Neilson, A.B. and Holder, A.J. 2000. Gaussview user Manual, Gaussian Inc., Pittsburgh, PA.

Frisch, MJ., Trucks, GW., Schlegel, HB, *et al.,* 2004. Gaussian 03. Gaussian Inc, Wallingford CT.

Hirsinger, L. and Lexcellen, C. 2003. Internal variable model for magneto-mechanical behaviour of ferromagnetic shape memory alloys Ni-Mn-Ga., *Journal of Physics,* IV, 112, pp 977.

Kraus, W. and Nolze (BAM Berlin), Powder Cell 2.4, Federal Institute of Materials Research and Testing, Unter den Eichen 87, D-12205 Berlin.

Manickam Mahendran, 2005. Microstructural analysis and phase transformation in Ni–Mn–Ga ferromagnetic shape memory alloys, Smart Material Structure, 14, pp 1403–1409.

Murray, SJ., Marioni, MA., Allen, SM., O'Handley, RC. And Lograsso, TA. 2000. 6% magnetic-field-induced strain by twin-boundary motion in ferromagnetic Ni–Mn–Ga, *Applied Physics Letter,* 77, pp 886-889.

O'Handley, R.C., Paul, D.I., Allen, S.M., Richard, M., Feuchtwanger, J., Peterson, B., Techapiesancharoenkij, R., Barandiar´an, M. and L´azpita, P. 2006. Model for temperature dependence of field-induced strain in ferromagnetic shape memory alloys. *Materials Science and Engineering* A, 438 , pp 445–449.

Ozdemir Kart, S., Uludogan, M., Karaman, I. and Cagın, T. 2008. DFT Studies on Structure, Mechanics and Phase Behavior of Magnetic Shape Memory Alloys: Ni_2MnGa. *Physica Status Solidi,* 205: 1026–1035.

Sarawate, N.N. and Dapino, M. J. 2007. A continuum thermodynamics model for the sensing effect in ferromagnetic shape memory Ni–Mn–Ga. *Journal of Applied Physics,* 101, pp 123522 -11.

Singh, R.K. and Gopalan, R. 2008. Martensite transformation and magnetic property dependence on the annealing temperature in Ni-rich Ni-Mn-Ga alloy. *Advanced Materials Research,* 52 , pp 57-62.

Singh, R.K., Shamsuddin, M., Gopalan, R., Mathur, R.P. and Chandrasekaran, V. 2008. Magnetic and structural transformation in off-stoichiometric NiMnGa alloys. *Materials Science and Engineering*, A476, pp 195–200.

Sozinov, A., Likhachev, A.A., Lanska, N. and Ullakko, K. 2002. Giant magnetic- field-induced strain in NiMnGa seven-layered martensitic phase. *Applied Physics Letter*, 80, pp 1746-1748.

Ullakko, K., Huang, J.K., Kantner, C., O'Handley, R.C. and Kokorin, V.V. 1996. Large magnetic-field-induced strains in Ni_2MnGa single crystals. *Applied Physics Lette*r, 69, pp 1966-68.

Wan, J.F. and Wang, J.N. 2005. Structure dependence of optical spectra of ferromagnetic Heusler alloy Ni–Mn–Ga, Physica B, 355, pp 172-175.

Wedel. K., Suzuki, M., Murakami, Y., Wedel, C., Suzuki, T., Shindo, K.D. and Itagaki, K. 1999. Crystal Structure of Ni—Mn—Ga Alloys. *Journal of Alloys and Compound*s, 290, pp 137.

****